PROCEEDINGS OF SCIENCE

F-Term Hybrid Inflation, Metastable Cosmic Strings and Low Reheating in View of ACT

C. Pallis[a,*]

[a] *School of Civil Engineering,*
Faculty of Engineering,
Aristotle University of Thessaloniki,
GR-541 24 Thessaloniki, GREECE

E-mail: kpallis@auth.gr

We consider the formation of metastable cosmic strings in a left-right unified theory. The produced monopoles are diluted by a stage of F-term hybrid inflation (FHI) which is realized consistently with the SUSY breaking and a global $U(1)$ R symmetry in the context of a $U(1)_{\rm R}\times U(1)_{B-L}$ extension of MSSM. The hidden sector Kähler manifold enjoys an enhanced $SU(1,1)/U(1)$ symmetry with the scalar curvature determined by the achievement of a SUSY-breaking de Sitter vacuum without ugly tuning. FHI turns out to be compatible with data – including the recent ACT results –, provided that the magnitude of the emergent soft tadpole term is confined in the range $(0.1-70)$ TeV, and it is accompanied with the production of cosmic strings. Their dimensionless tension $G\mu_{\rm cs}\simeq(1-11)\cdot10^{-8}$ interprets the present observations from PTA experiments on the stochastic background of gravitational waves. The μ parameter of MSSM arises by appropriately adapting the Giudice-Masiero mechanism and facilitates the out-of-equilibrium decay of the R saxion at a reheat temperature lower than about 34 GeV. The SUSY mass scale turns out to lie in the PeV region.

Proceedings of the Corfu Summer Institute 2024 "School and Workshops on Elementary Particle Physics and Gravity" (CORFU2024)
12 - 26 May, and 25 August - 27 September, 2024
Corfu, Greece

*Speaker

 ISSN 1824-8039 . Published by SISSA Medialab.

PoS(CORFU2024)206

1. Introduction

In this talk we attempt to bring together the recent data [1, 2] on *gravitational waves* (GWs), inflation [3, 4] and *Supersymmetry* (SUSY) breaking [5]. The junction point is the metastable *cosmic strings* (CSs) [6] whose decay interprets the recent data on GWs. Their generation requires a specific GUT construction – see Sec. 1.1 – in conjunction with a suitable inflationary stage – see Sec. 1.2.

1.1 PTA Data and Metastable CSs

The discovery of a background of GWs around the nanohertz frequencies announced from several *Pulsar Timing Array* (PTA) experiments [1] – most notably the *NANOGrav 15-years results* (NG15) – provides a novel tool in exploring the structure of early universe. The observations can be explained by gravitational radiation emitted by topologically unstable superheavy CSs which may be formed during the *spontaneous symmetry breaking* (SSB) chains of *Grand Unified Theories* (GUTs) [7] down to the *Standard Model* (SM) gauge group $\mathbb{G}_{\rm SM}$. In particular, the observations can be interpreted if the CSs are metastable. This type of CSs arise from a SSB of the form

$$\mathbb{G} \xrightarrow[\text{MMs}]{\langle \text{adj}(\mathbb{G})\rangle} \mathbb{G}_{\rm int}\times U(1) \xrightarrow[\text{CSs}]{} \mathbb{G}_{\rm f} \text{ with } \pi_1(\mathbb{G}/\mathbb{G}_{\rm int}) = \pi_1(\mathbb{G}/\mathbb{G}_{\rm f}) = I \neq \pi_1(\mathbb{G}_{\rm int}\times U(1)/\mathbb{G}_{\rm f}). \quad (1)$$

Here MMs stands for *Magnetic Monopoles* and adj($\mathbb{G}$) for the adjoint representation of $\mathbb{G}_{\rm GUT}$. Also π_n is the $n^{\rm th}$ homotopy group. MMs are produced at the first stage of the chain above since we expect

$$\pi_2(\mathbb{G}/\mathbb{G}_{\rm int}\times U(1)) \neq I.$$

The simplest way to implement such a SSB in a realistic particle model is to identify

$$\mathbb{G} = SU(2)_{\rm R}\times U(1)_{B-L} \text{ and } \mathbb{G}_{\rm int}\times U(1) = U(1)_{\rm R}\times U(1)_{B-L}. \quad (2)$$

Here $\mathbb{G}$ may be embedded in the well-known Left-Right gauge group – cf. Ref. [8, 9]

$$\mathbb{G}_{\rm LR} := SU(3)_{\rm C}\times SU(2)_{\rm L}\times SU(2)_{\rm R}\times U(1)_{B-L} \quad (3)$$

and so adj($\mathbb{G}$) may be identified by $(\mathbf{1},\mathbf{1},\mathbf{3},0)$. Since the production of MMs is cosmologically catastrophic, these are to be inflated away. However, they can appear on CSs via quantum pair creation if the formatted CSs are metastable.

1.2 CSs, Inflation and ACT Data

A well-motivated inflationary model, which may dilute MMs and is naturally followed by a GUT phase transition possibly leading to the formation of CSs is *F-term hybrid inflation* FHI [10] – for reviews see Ref. [11, 12]. Therefore, we consider the implementation of FHI within the gauge group

$$\mathbb{G}_{\rm L1R} := SU(3)_{\rm C}\times SU(2)_{\rm L}\times U(1)_{\rm R}\times U(1)_{B-L} \quad (4)$$

which results after the SSB of $\mathbb{G}_{\rm LR}$ from the *vacuum expectation value* (v.e.v) $\langle(\mathbf{1},\mathbf{1},\mathbf{3},0)\rangle := v_{\rm R}$.

For a reliable approach to FHI, soft SUSY-breaking terms and *Supergravity* (SUGRA) corrections have to be taken into account together with the *radiative corrections* (RCs) employed in the

original version of the model [10]. Both former corrections above are of crucial importance in order to reconcile the inflationary observables with data [13–16] and are obviously related to the adopted SUSY-breaking sector. Following Ref. [17, 18] we here update – in the light of *Atacama Cosmology Telescope* (ACT) results [4] – the combination of FHI and SUSY breaking using as a junction mechanism of the (visible) *inflationary sector* (IS) and the *hidden sector* (HS) a mildly violated R symmetry [19] – not to be confused with the gauge $SU(2)_{\rm R}$ or $U(1)_{\rm R}$ symmetries included in $\mathbb{G}_{\rm LR}$ and $\mathbb{G}_{\rm L1R}$, see Eqs. (3) and (4) respectively.

Schematically, the steps of SSB in our setting can be demonstrated as follows

$$\begin{aligned}\mathbb{G}_{\rm LR}\times U(1)_R\times U(1)_B\times{\rm SUGRA}\ &\xrightarrow[\text{MMs}]{\langle(\mathbf{1},\mathbf{1},\mathbf{3},0)\rangle=v_{\rm R}}\ \mathbb{G}_{\rm L1R}\times U(1)_R\times U(1)_B\times{\rm SUGRA}\\ &\xrightarrow[\langle Z\rangle,\ \text{CSs}]{\text{(FHI)}\ \langle\bar\Phi\rangle=\langle\Phi\rangle=M}\ \mathbb{G}_{\rm SM}\times\mathbb{Z}_2^R\times U(1)_B\times\not{\rm SUSY}\\ &\xrightarrow[\text{RCs}]{\langle H_d\rangle,\langle H_u\rangle}\ SU(3)_{\rm C}\times U(1)_{\rm EM}\times U(1)_B,\end{aligned}\tag{5}$$

where we include also the final transition to the present vacuum which occurs via the well-known radiative electroweak SSB – EM stands for *ElectroMagnetism*. Contrary to Ref. [20, 21] we do not specify the dynamics of the SSB of $\mathbb{G}_{\rm LR}$ but we incorporate the mechanism of SUSY breaking as shown in the rightmost part of the second line. Note that soft SUSY breaking effects explicitly break $U(1)_R$ to the $\mathbb{Z}_2^R$ which remains unbroken and, if combined with the fermion parity, yields the well-known R-parity of MSSM.

We describe in Sec. 2 below our model. Then, we analyze the inflationary – see Sec. 3 – and the post-inflationary – see Sec. 4 – stage of the cosmological evolution within our setting. The spectrum of GWs obtained by the CSs within our framework is presented in Sec. 5. Our conclusions are summarized in Sec. 6.

2. Particle Model

Here we determine the particle content, the superpotential, and the Kähler potential of our model. These ingredients are presented in Secs. 2.1, 2.2 and 2.3.

2.1 Particle Content

As already mentioned, we focus on the second line of Eq. (5) and therefore we consider a model invariant under the gauge group $\mathbb{G}_{\rm L1R}$ in Eq. (4) which incorporates FHI. In addition to the local symmetry, the model possesses the baryon and lepton number symmetries and an R symmetry $U(1)_R$. The representations under $\mathbb{G}_{\rm L1R}$ and the charges under the global symmetries of the various matter and Higgs superfields of the model are presented in Table 1. Namely, the ith generation $SU(2)_{\rm L}$ doublet left-handed quark and lepton superfields are denoted by q_i and l_i respectively, whereas the $SU(2)_{\rm L}$ singlet antiquark [antilepton] superfields by u_i^c and $d_i{}^c$ [e_i^c and ν_i^c] respectively. The electroweak Higgs superfields which couple to the up [down] quark superfields are denoted by H_u [H_d]. Besides the MSSM particle content, the model is augmented by seven superfields: a gauge singlet S, three ν_i^c's, a pair of Higgs superfields Φ and $\bar\Phi$ which break

Super-fields	Representations under $\mathbb{G}_{\rm L1R}$	Global Symmetries		
		R	B	L
Matter Superfields				
l_i	$(\mathbf{1},\mathbf{2},0,-1)$	0	0	1
e_i^c	$(\mathbf{1},\mathbf{1},1/2,1)$	0	0	-1
ν_i^c	$(\mathbf{1},\mathbf{1},-1/2,1)$	0	0	-1
q_i	$(\mathbf{3},\mathbf{2},0,1/3)$	0	$1/3$	0
u_i^c	$(\bar{\mathbf{3}},\mathbf{1},1/2,-1/3)$	0	$-1/3$	0
d_i^c	$(\bar{\mathbf{3}},\mathbf{1},-1/2,-1/3)$	0	$-1/3$	0
Higgs Superfields				
H_d	$(\mathbf{1},\mathbf{2},-1/2,0)$	2	0	0
H_u	$(\mathbf{1},\mathbf{2},1/2,0)$	2	0	0
S	$(\mathbf{1},\mathbf{1},0,0)$	2	0	0
Φ	$(\mathbf{1},\mathbf{1},-1/2,1)$	0	0	-2
$\bar{\Phi}$	$(\mathbf{1},\mathbf{1},1/2,-1)$	0	0	2
Goldstino Superfield				
Z	$(\mathbf{1},\mathbf{1},0,0)$	$2/\nu$	0	0

Table 1: *The representations under $\mathbb{G}_{\rm L1R}$ and the extra global charges of the superfields of our model.*

$U(1)_{\rm R}\times U(1)_{B-L}$ and the goldstino superfield Z. Note that the SM hypercharge Q_Y is identified as the linear combination $Q_Y = Q_{\rm R} + Q_{(B-L)}/2$ where $Q_{\rm R}$ and $Q_{(B-L)}$ is the $U(1)_{\rm R}$ and $B-L$ charge respectively.

2.2 Superpotential

The superpotential of our model respects totally the symmetries in Table 1. Most notably, it carries R charge 2 and is linear *with respect to* (w.r.t.) S and Z^ν. It naturally splits into five parts:

$$W = W_{\rm I} + W_{\rm H} + W_{\rm GH} + W_{\rm MSSM} + W_{\rm MD}, \tag{6}$$

where the subscripts "I" and "H" stand for IS and HS respectively and the content of each term is specified as follows:

(a) $W_{\rm I}$ includes the terms of the IS of model [10]

$$W_{\rm I} = \kappa S\left(\bar{\Phi}\Phi - M^2\right), \tag{7a}$$

where κ and M are free parameters which may be made positive by field redefinitions.

(b) $W_{\rm H}$ depends on the HS and is written as [19]

$$W_{\rm H} = m m_{\rm P}^2 (Z/m_{\rm P})^\nu. \tag{7b}$$

Here $m_{\rm P} = 2.4$ ReV is the reduced Planck mass – with ReV $= 10^{18}$ GeV –, m is a positive free parameter with mass dimensions, and ν is an exponent which may, in principle, acquire any real value if we consider $W_{\rm H}$ as an effective superpotential valid close to the non-zero v.e.v of Z, $\langle Z\rangle$.

(c) $W_{\rm GH}$ mixes the HS and the gauge fields of the IS. It has the form

$$W_{\rm GH} = -\lambda m_{\rm P}(Z/m_{\rm P})^{\nu}\bar{\Phi}\Phi \tag{7c}$$

with λ a real coupling constant.

(d) $W_{\rm MSSM}$ contains the usual trilinear terms of MSSM, i.e.,

$$W_{\rm MSSM} = h_{ijD}d_i^c q_j H_d + h_{ijU}u_i^c q_j H_u + h_{ijE}e_i^c l_j H_d. \tag{7d}$$

The selected R assignments in Table 1 prohibit the presence in $W_{\rm MSSM}$ of the bilinear $\mu H_u H_d$ term of MSSM and other unwanted mixing terms – e.g. $\lambda_\mu S H_u H_d$.

(e) $W_{\rm MD}$ provides masses to neutrinos, i.e.,

$$W_{\rm MD} = h_{ij\nu}\nu_i^c l_j H_u + \lambda_{iN^c}\left(S/m_{\rm P} + (Z/m_{\rm P})^{\nu}\right)\left(\bar{\Phi}\nu_i^c\right)^2/m_{\rm P}. \tag{7e}$$

The first term in the right-hand side of Eq. (7e) is responsible for Dirac neutrino masses whereas the third one – given that $\langle S\rangle = 0$ as we see in Sec. 4.1 below – for the Majorana masses – cf. Refs. [14, 18]. The scale of the latter masses is intermediate since $\langle\bar{\Phi}\rangle \sim 1$ YeV and $\langle Z\rangle \sim m_{\rm P}$. The cooperation of both terms lead to the light neutrino masses via the well-known (type I) seesaw mechanism.

2.3 Kähler Potential

The Kähler potential respects the $\mathbb{G}_{\rm L1R}$, B and L symmetries in Table 1 and breaks mildly the R symmetry. It includes the following contributions

$$K = K_{\rm I} + K_{\rm H} + K_\mu + |Y_\alpha|^2, \tag{8}$$

where the left-handed chiral superfields of MSSM are denoted by Y_α with $\alpha = 1, ..., 20$, i.e.,

$$Y_\alpha = l_i, {e_i}^c, \nu_i^c, q_i, {d_i}^c, {u_i}^c, H_d \text{ and } H_u.$$

The individual contributions into K can be specified as follows:

(a) $K_{\rm I}$ depends on the fields involved in IS – cf. Eq. (7a). We adopt the simplest possible choice – cf. Ref. [12, 14] – which has the form

$$K_{\rm I} = |S|^2 + |\Phi|^2 + |\bar{\Phi}|^2 \tag{9a}$$

and has zero contribution into the quadratic correction to the inflationary potential – see Sec. 3.2 below.

(b) $K_{\rm H}$ is devoted to HS. We adopt the form introduced in Ref. [19] where

$$K_{\rm H} = N m_{\rm P}^2 \ln\left(1 + \frac{|Z|^2 - k^2 Z_-^4/m_{\rm P}^2}{N m_{\rm P}^2}\right) \quad \text{with} \quad Z_\pm = Z \pm Z^*. \tag{9b}$$

Here, $k > 0$ mildly violates the R symmetry endowing R axion with phenomenologically acceptable mass. The selected form of $K_{\rm H}$ ensures – as we see in Sec. 4.1 – a de Sitter vacuum of the whole field system with tunable cosmological constant for

$$N = \frac{4\nu^2}{3-4\nu} \quad \text{with} \quad \frac{3}{4} < \nu < \frac{3}{2} \quad \text{for} \quad N < 0. \tag{10}$$

Our favored ν range finally is $3/4 < \nu < 1$. Since $N < 0$, $K_{\rm H}$ parameterizes the $SU(1,1)/U(1)$ hyperbolic Kähler manifold for $k \sim 0$.

(c) K_μ includes higher order terms which generate the needed mixing term between H_u and H_d in the lagrangian of MSSM [19] and has the form

$$K_\mu = \lambda_\mu \left(Z^*/m_{\rm P}\right)^{2\nu} H_u H_d \ + \ \text{h.c.}, \tag{11}$$

where the dimensionless constant λ_μ is taken real for simplicity.

The total K in Eq. (8) enjoys an enhanced symmetry for the $\bar{Y}^A$ and Z fields where $A = \alpha, \bar{\Phi}, \Phi, S$. Namely, this symmetry can be written as

$$\prod_A U(1)_{\bar{Y}^A} \times \left(SU(1,1)/U(1)\right)_Z , \tag{12}$$

where the indices indicate the moduli which parameterize the corresponding manifolds. Thanks to this symmetry, mixing terms allowed by the R symmetry can be ignored.

3. Inflation Analysis

It is well known [10] that in global SUSY FHI takes place for sufficiently large $|S|$ values along a F- and D- flat direction of the SUSY potential

$$\bar{\Phi} = \Phi = 0, \ \ \text{where} \ \ V_{\rm SUSY}\left(\Phi = 0\right) := V_{\rm I0} = \kappa^2 M^4 \ \ \text{and} \ \ H_{\rm I} = \sqrt{V_{\rm I0}/3m_{\rm P}^2} \tag{13}$$

are the constant potential energy density and correspoding Hubble parameter which drive FHI – the subscript 0 means that this is the tree level value. In the present context, though, prominent role in the investigation plays the F-term SUGRA potential $V_{\rm F}$ which is minimized under the conditions displayed in Sec. 3.1 and then in Sec. 3.2 we give the final form of the inflationary potential. Lastly, we present our results in Sec. 3.4 imposing a number of constraints listed in Sec. 3.3.

3.1 Hidden Sector's Stabilization

If we analyze S and Z as follows

$$S = \sigma\, e^{i\theta_S/m_{\rm P}}/\sqrt{2} \ \text{ and } \ Z = (z + i\theta)/\sqrt{2}, \tag{14}$$

we can show [17] that $V_{\rm F}$ is minimized along the inflationary trajectory in Eq. (13) for

$$\langle\theta_S\rangle_{\rm I} = \langle\theta\rangle_{\rm I} = 0 \ \text{ and } \ \langle z\rangle_{\rm I} \simeq \left(\sqrt{3}\cdot 2^{\nu/2-1} H_{\rm I}/m\nu\sqrt{1-\nu}\right)^{1/(\nu-2)} m_{\rm P}. \tag{15}$$

Note that $\nu < 1$ assures a real value of $\langle z\rangle_{\rm I}$ with $\langle z\rangle_{\rm I} \ll m_{\rm P}$ since $H_{\rm I}/m \ll 1$.

The (canonically normalized) components of sgoldstino, acquire masses squared, respectively,

$$m^2_{{\rm I}z} \simeq 6(2-\nu)H^2_{\rm I} \ \text{ and } \ m^2_{{\rm I}\theta} \simeq 3H^2_{\rm I} - m^2\left(8\nu^2 m^2_{\rm P} - 3\langle z\rangle^2_{\rm I}\right)\frac{4\nu(1-\nu)m^2_{\rm P} + (1-96k^2\nu)\langle z\rangle^2_{\rm I}}{2^{3+\nu}\nu m^{2\nu}_{\rm P}\langle z\rangle^{2(2-\nu)}_{\rm I}}, \tag{16a}$$

whereas the mass of $\widetilde{G}$ turns out to be

$$m_{\rm I3/2} \simeq \left(\nu(1-\nu)^{1/2} m^{2/\nu}/\sqrt{3}H_{\rm I}\right)^{\nu/(2-\nu)}. \tag{16b}$$

For the benchmark point presented in Table 2 we can numerically verify that $m_{{\rm I}z} \gg H_{\rm I}$ and $m_{{\rm I}\theta} \simeq H_{\rm I}$ given that $H_{\rm I} = 1.05$ EeV consistently with the inflationary requirements in Sec. 3.2. Therefore, isocurvature perturbations do not constrain the parameters [17].

3.2 Inflationary Potential

Expanding $V_{\rm F}$ for low S values, introducing the canonically normalized inflaton $\sigma = \sqrt{2}|S|$ and taking into account the RCs [10] we derive [17] the inflationary potential $V_{\rm I}$ which can be cast in the form

$$V_{\rm I} \simeq V_{\rm I0}\left(1 + C_{\rm RC} + C_{\rm SSB} + C_{\rm SUGRA}\right), \ \text{ where} \tag{17}$$

(a) $C_{\rm RC}$ includes the RCs which may be written as [10–12]

$$C_{\rm RC} = \frac{\kappa^2}{128\pi^2}\left(8\ln\frac{\kappa^2 M^2}{Q^2} + 8x^2\tanh^{-1}\left(\frac{2}{x^2}\right) - 4(\ln 4 - x^4\ln x) + (4+x^4)\ln(x^4-4)\right) \tag{18a}$$

with $x = \sigma/M > \sqrt{2}$. For $x \leq \sqrt{2}$, the path in Eq. (13) develops a tachyonic instability occurs in the mass spectrum of the $\bar{\Phi} - \Phi$ system triggering thereby the $U(1)_{\rm R}\times U(1)_{B-L}$ phase transition which generates the desired CSs.

(b) $C_{\rm SSB}$ comes from the soft SUSY-breaking effects [13] and can be parameterized as follows:

$$C_{\rm SSB} = m^2_{\rm I3/2}\frac{\sigma^2}{2V_{\rm I0}} - {\rm a}_S\frac{\sigma}{\sqrt{2V_{\rm I0}}} \ \text{ with } \ {\rm a}_S = 2^{1-\nu/2} m\frac{\langle z\rangle^\nu_{\rm I}}{m^\nu_{\rm P}}\left(1 + \frac{\langle z\rangle^2_{\rm I}}{2Nm^2_{\rm P}}\right)\left(2 - \nu - \frac{3\langle z\rangle^2_{\rm I}}{8\nu m^2_{\rm P}}\right) \tag{18b}$$

the tadpole parameter. In the expression above, we take care to minimize $V_{\rm I}$ w.r.t θ_S in Eq. (14) which is assumed to be constant during FHI – cf. Ref. [15].

Model Parameters			
$\lambda/10^{-12}$	M/YeV	m/PeV	α_s/TeV
1.4	2.3	3.5	25.6
HS Parameters During FHI			
$\langle z\rangle_I/10^{-3}m_P$	m_{Iz}/EeV	$m_{I\theta}$/EeV	$m_{I3/2}$/EeV
2	2.7	0.5	11.2
Quantities Related to FHI			
$\sigma_\star/\sqrt{2}M$	$\alpha_s/10^{-4}$	$r/10^{-11}$	$G\mu_{cs}/10^{-8}$
1.097	−2.3	2.5	7.4
Spectrum at the Vacuum			
m_I/ZeV	m_z/PeV	m_θ/PeV	$m_{3/2}$/PeV
5.2	6.2	8.8	5.6
Reheat Temperature T_{rh}/GeV			
For $\mu/\widetilde{m}=3$		For $\mu/\widetilde{m}=1/3$	
3		0.4	

Table 2: *Parameters and quantities of interest for our model with fixed* $\kappa = 0.001$, $\nu = 7/8$ *and* $k = 0.1$ *resulting to* $n_s = 0.974$ *for* $N_{I\star} \simeq 41$ *– recall that* 1 YeV = 10^3 ZeV = 10^6 EeV = 10^9 PeV = 10^{15} GeV.

(c) C_{SUGRA} is the remaining – i.e., after subtracting C_{SSB} – SUGRA correction, which is

$$C_{SUGRA} = c_{2\nu}\frac{\sigma^2}{2m_P^2} + c_{4\nu}\frac{\sigma^4}{4m_P^4} \text{ with } c_{2\nu} = \frac{\langle z\rangle_I^2}{2m_P^2} \text{ and } c_{4\nu} = \frac{1}{2}\left(1 + \frac{\langle z\rangle_I^2}{m_P^2}\right). \tag{18c}$$

FHI is feasible thanks to the stabilization of z in Eq. (15) to low enough values and the minimality of K_I in Eq. (9a) which offers the magic cancellation [12] of the quadratic correction in C_{SUGRA}.

3.3 Observational Requirements

The inflationary part of our setting can be constrained by imposing the following observational requirements:

(a) The number of e-foldings elapsed from horizon exit of $k_\star = 0.05/\text{Mpc}$ k until the end of inflation at $\sigma_f \simeq \sigma_c$ have to be enough to resolve the problems of the Standard Big Bang, i.e., [3]:

$$N_{I\star} = -\int_{\sigma_\star}^{\sigma_f} \frac{d\sigma}{m_P^2}\frac{V_I}{V_I'} \simeq 41 + \frac{2}{3}\ln\frac{V_{I0}^{1/4}}{0.1\text{ YeV}} + \frac{1}{3}\ln\frac{T_{rh}}{1\text{ GeV}}, \tag{19}$$

where the prime denotes derivation w.r.t. σ and $\sigma_\star$ is the value of σ when $k_\star$ crosses outside the horizon of FHI. Here, we have assumed that the "reheating temperature" due to the decay of IS after FHI is lower than ρ_{zI}– see Eq. (29) below – and, thus, we obtain just matter domination after the end of FHI and before the complete decay of $\widehat{\delta z}$ which yields the correct reheating temperature $T_{rh} \sim 1$ GeV.

(b) The amplitude $A_{\rm s}$ of the power spectrum of the curvature perturbation generated by σ during FHI must be appropriately normalized [4] , i.e.,

$$\sqrt{A_{\rm s}} = \frac{1}{2\sqrt{3}\pi m_{\rm P}^3}\,\frac{V_{\rm I}^{3/2}(\sigma_\star)}{|V_{\rm I}'(\sigma_\star)|} \simeq 4.618\cdot 10^{-5}. \tag{20}$$

(c) The remaining observables – the scalar spectral index $n_{\rm s}$, its running $\alpha_{\rm s}$, and the scalar-to-tensor ratio r – which are calculated by the following standard formulas

$$n_{\rm s} = 1 - 6\epsilon_\star + 2\eta_\star, \alpha_{\rm s} = 2\left(4\eta_\star^2 - (n_{\rm s}-1)^2\right)/3 - 2\xi_\star \text{ and } r = 16\epsilon_\star \tag{21}$$

(where $\xi \simeq m_{\rm P}^4\, V_{\rm I}' V_{\rm I}'''/V_{\rm I}^2$ and all the variables with the subscript $\star$ are evaluated at $\sigma = \sigma_\star$) must be in agreement with the combination of *Planck*, ACT, DESI and BICEP/*Keck* telescopes (P-ACT-LB-BK18) data, i.e., [4]

$$n_{\rm s} = 0.974 \pm 0.0068 \text{ and } r \lesssim 0.038 \tag{22}$$

at 95% *confidence level* (c.l.) with negligible $|\alpha_{\rm s}| \ll 0.01$.

3.4 Results

The inflationary part of our model depends on the parameters – cf. Ref. [14] – κ, M and a_S, where a_S can be derived from m and ν via the rightmost relation in Eq. (18b). Enforcing Eqs. (19) and (20) we can restrict M and $\sigma_\star$ as functions of κ and a_S. On the other hand, the correct $n_{\rm s}$ values in Eq. (22) are attained if FHI becomes of hilltop type [14, 15] via a careful selection of a_S. I.e., $V_{\rm I}$ is non-monotonic and develops a maximum at $\sigma_{\rm max}$ and a minimum at $\sigma_{\rm min} \gg \sigma_{\rm max}$. For $\sigma > \sigma_{\rm min}$, $V_{\rm I}$ becomes a monotonically increasing function of σ and so its boundedness is assured. FHI takes place for $\sigma < \sigma_{\rm max}$. The achievement of successful hilltop FHI requires the establishment of the hierarchy $\sigma_{\rm c} < \sigma_\star < \sigma_{\rm max}$. As a consequence, the obtained $n_{\rm s}$ values decline from the prediction $n_{\rm s} \simeq 1 - 1/N_{{\rm I}\star}$ of the original model [10, 16] which provides the correct value in Eq. (22), though, for the $N_{{\rm I}\star} \sim 41$.

The parameter space of our model allowed by the inflationary requirements in Eqs. (19), (20) and (22) is delineated in Fig. 1 where we present the gray shaded regions in the $\kappa - a_S$ and $M - a_S$ plane – see Fig. 1-(a) and Fig. 1-(b) respectively. The boundaries of the allowed areas are determined by the dashed [dot-dashed] line corresponding to the upper [lower] bound on $n_{\rm s}$ in Eq. (22). We also display by solid lines the allowed contours for the central value of $n_{\rm s}$ in Eq. (22). The maximal r's are encountered in the upper right end of the dashed lines – corresponding to $n_{\rm s} = 0.981$. On the other hand, the maximal $|\alpha_{\rm s}|$'s are achieved along the dot-dashed lines and the minimal value is $\alpha_{\rm s} = -3.2\cdot 10^{-4}$. Summarizing our findings from Fig. 1 for central $n_{\rm s}$ in Eq. (22) we end up with the following ranges:

$$0.84 \lesssim M/{\rm YeV} \lesssim 2.72,\ \ 2 \lesssim \kappa/10^{-4} \lesssim 14 \text{ and } 0.11 \lesssim a_S/{\rm TeV} \lesssim 70. \tag{23}$$

The lower bounds of these inequalities are expected to be displaced to slightly larger values due to the constraints in Eq. (31) – see Sec. 4.2 below – which are not considered here for the shake of generality.

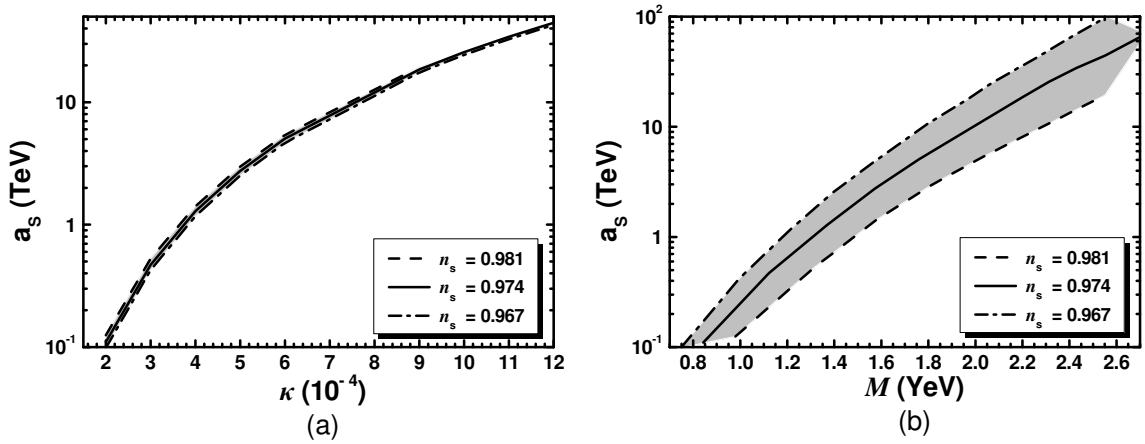

Figure 1: *Allowed (shaded) regions as determined by Eqs. (19), (20) and (22) in the $\kappa - a_S$ (a) and $M - a_S$ (b). The conventions adopted for the various lines are also shown.*

4. Post-Inflationary Era

The coupling of HS to IS not only explains the appearance of the terms $C_{\rm SSB}$ and $C_{\rm SUGRA}$ in $V_{\rm I}$ but also has far-reaching consequences regarding the problem of DE, the reheating in our scenario and the SUSY-mass scale. These issues are analyzed in Sec. 4.1, 4.2 and 4.3 below.

4.1 SUSY and $\mathbb{G}_{\rm L1R}$ Breaking

The minimization of the F–term (tree level) SUGRA scalar potential $V_{\rm F}$ [17], which includes contributions from both the HS and the IS, yields the vacuum of our model which is determined by the conditions

$$|\langle\Phi\rangle| = \left|\langle\bar{\Phi}\rangle\right| = M, \;\; \langle\sigma\rangle \simeq 2^{(1-\nu)/2}\,(m-\lambda m_{\rm P})\;\; z^{\nu}/m_{\rm P}^{\nu} \;\; \text{and} \;\; \langle z\rangle = 2\sqrt{2/3}|\nu|m_{\rm P} \tag{24}$$

with $\langle\theta\rangle = \langle\theta_S\rangle = 0$. Contrary to the status in the absence of IS [19], the vacuum potential energy density here is not zero but constant with value

$$\langle V_{\rm F}\rangle = \left(\frac{16\nu^4}{9}\right)^{\nu}\left(\frac{\lambda M^2 - m m_{\rm P}}{\kappa m_{\rm P}^2}\right)^2 \omega^N m_{\rm P}^2\,(\lambda m_{\rm P} - m)^2 \;\; \text{with} \;\; \omega \simeq \frac{2(3-2\nu)}{3}. \tag{25}$$

Tuning λ to a value $\lambda \sim m/m_{\rm P} \simeq 10^{-12}$ we may wish identify $\langle V_{\rm F}\rangle$ with the DE energy density [4]

$$\langle V_{\rm F}\rangle \simeq 10^{-120} m_{\rm P}^4. \tag{26}$$

Therefore, we obtain a dS vacuum with $\langle\sigma\rangle \simeq 0$ which resolves without extensive tuning the notorious DE problem. At this vacuum we can estimate the masses of the gravitino, the sgoldstino (or R saxion), the pseudo-sgoldstino (or R axion) and the IS which are respectively [19]

$$m_{3/2} \simeq 2^{\nu}3^{-\nu/2}|\nu|^{\nu} m\omega^{N/2},\; m_z \simeq \frac{3\omega}{2\nu}m_{3/2},\; m_\theta \simeq 12k\omega^{3/2}m_{3/2} \tag{27a}$$

$$\text{and} \;\; m_{\rm I} = e^{K_{\rm H}/2m_{\rm P}^2}\sqrt{2}\left(\kappa^2 M^2 + (4\nu^2/3)^{\nu}(1+4M^2/m_{\rm P}^2)m^2\right)^{1/2}. \tag{27b}$$

Typical values for the masses above are given in Table 2, where we see that besides $m_{\rm I}$, which is of order 1 ZeV, the other masses are of order 1 PeV.

At the vacuum of Eq. (24) K_μ in Eq. (11) gives rise to a non-vanishing μ term in the superpotential whereas the contributions $W_{\rm MSSM}$ and $|Y_\alpha|^2$ of W and K in Eqs. (6) and (8) lead to a common soft SUSY-breaking mass parameter $\widetilde{m}$. Namely, we obtain [17, 19]

$$W \ni \mu H_u H_d \;\; \text{with} \;\; |\mu| = \lambda_\mu \left(4\nu^2/3\right)^\nu (5-4\nu) m_{3/2} \;\; \text{and} \;\; \widetilde{m} = m_{3/2}. \tag{28}$$

The latter quantity indicatively represents the mass level of the SUSY partners and allows us to connect the inflationary model with the SUSY phenomenology via Eqs. (18b) and (23) – see below.

4.2 Low Reheating

Soon after FHI, the IS and $\widehat{\delta z}$ enter into an oscillatory phase about their minima in Eq. (24) and eventually decay. Due to the large $\langle z\rangle \sim m_{\rm P}$ in Eq. (24), the energy density of the z condensate at the onset of oscillations, $\rho_{z\rm I}$, – when $H_{z\rm I} \sim m_z$ – dominates the corresponding universal energy density $\rho_{z\rm It}$. Indeed,

$$\rho_{z\rm I} \sim m_z^2 \langle z\rangle^2 \sim m_z^2 m_{\rm P}^2 \;\; \text{and} \;\; \rho_{z\rm It} = 3 m_{\rm P}^2 H_{z\rm I}^2 \simeq 3 m_{\rm P}^2 m_z^2. \tag{29}$$

Due to weakness of the z interactions, the reheating temperature which is determined by the decay width of $\widehat{\delta z}$, $\Gamma_{\delta z}$, is quite suppressed – see values of Table 2 for two extremal $\mu/m_{3/2}$ values. Indeed,

$$T_{\rm rh} = \left(72/5\pi^2 g_{\rm rh*}\right)^{1/4} \Gamma_{\delta z}^{1/2} m_{\rm P}^{1/2}, \;\; \text{with [17]} \;\; \Gamma_{\delta z} \sim \lambda_\mu^2 m_z^3/m_{\rm P}^2 \;\; \text{and} \;\; g_{\rm rh*} \simeq 10.75 - 100. \tag{30}$$

Here $\Gamma_{\delta z}$ is the decay width of $\widehat{\delta z}$ – cf. Ref. [23, 24] – and $g_{\rm rh*}$ counts the effective number of the relativistic degrees at $T_{\rm rh}$. This fact jeopardizes the successes of the standard *Big Bang Nucleosynthesis* (BBN) which requires [25]

$$T_{\rm rh} \geq 4.1 \,\text{MeV} \;\; \text{for} \;\; B_{\rm h} = 1 \;\; \text{and} \;\; T_{\rm rh} \geq 2.1 \,\text{MeV} \;\; \text{for} \;\; B_{\rm h} = 10^{-3}, \tag{31}$$

where $B_{\rm h}$ is the hadronic branching ratio and large $m_z \sim 0.1$ PeV is assumed. Moreover, in order to protect our setting from the so-called [26] moduli-induced $\widetilde{G}$ problem, we kinematically block the decay of $\widehat{\delta z}$ into $\widetilde{G}$'s selecting $\nu > 3/4$ which ensures $m_z < 2m_{3/2}$ – see Eq. (27a).

Taking κ and a_S – or m_z values via Eqs. (18b) and (27a) – allowed by the inflationary part of our model we find the allowed region in $\kappa - T_{\rm rh}$ plane, displayed in Fig. 2-(a), for $\nu = 7/8$. The boundary curves of the allowed region correspond to $\mu = \widetilde{m}/3$ or $\lambda_\mu = 0.22$ (dot-dashed line) and $\mu = 3\widetilde{m}$ or $\lambda_\mu = 1.96$ (dashed line). We see that there is an ample parameter space consistent with the BBN bounds depicted by two horizontal lines depending on the values of $B_{\rm h}$ in Eq. (31). The maximal value of $T_{\rm rh}$ for the selected ν is obtained for $\mu = 3\widetilde{m}$ and is estimated to be $T_{\rm rh}^{\rm max} \simeq 11$ GeV. Obviously, reducing μ below $\widetilde{m}/3$, the parameters λ_μ, $\Gamma_{\delta z}$ and so $T_{\rm rh}$ decrease too and the slice cut by the BBN bounds in Eq. (31) increases.

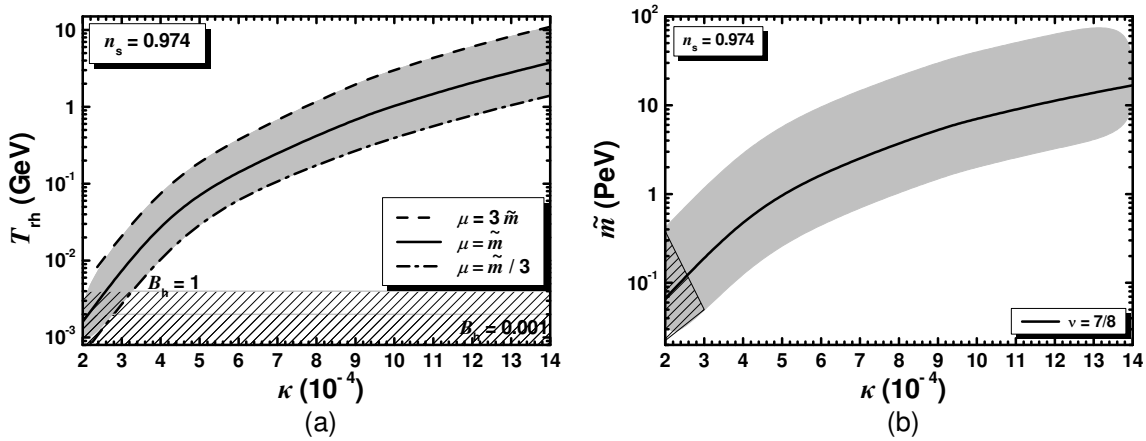

Figure 2: *Allowed (shaded) regions in the $\kappa - T_{\rm rh}$ (a) and $\kappa - \widetilde{m}$ (b) plane compatible with the inflationary requirements in Sec. 3.3 for $n_{\rm s} = 0.974$. We take (a) $\nu = 7/8$ and $\mu = \widetilde{m}$ (solid line), $\mu = \widetilde{m}/3$ (dot-dashed line) or $\mu = 3\widetilde{m}$ (dashed line) whereas the BBN lower bounds on $T_{\rm rh}$ for hadronic branching ratios $B_{\rm h} = 1$ and 0.001 are also depicted by two thin lines (b) $\widetilde{m}/3 \le \mu \le 3\widetilde{m}$ and $3/4 < \nu < 1$ whereas the allowed contour for $\nu = 7/8$ is depicted by a solid line and the region excluded by BBN for $B_{\rm h} = 0.001$ is hatched.*

4.3 SUSY-Mass Scale

As mentioned above, the restriction of the a_S values in Fig. 1 – see also Eq. (23) – via the attainment of successful FHI and the direct interconnection of a_S with m and $\widetilde{m}$ via Eqs. (18b) and (28) give us the opportunity to gain information about the mass scale of SUSY particles. Indeed, taking into account Eq. (15), which results to $\langle z\rangle_{\rm I}/m_{\rm P} \sim 10^{-3}$, and Eq. (23) we expect that $m \sim 1$ PeV and so $\widetilde{m} \sim 1$ PeV as well. This expectation is verified numerically in Fig. 2-(b), where we delineate the gray-shaded region allowed by the inflationary requirements of Sec. 3.3 for $n_{\rm s} = 0.974$ by varying ν and μ within their possible respective margins

$$0.75 < \nu < 1 \ \text{ and } \ 1/3 \lesssim \mu/\widetilde{m} \lesssim 3. \tag{32}$$

Obviously the lower boundary curve of the displayed region is obtained for $\nu \simeq 0.751$, whereas the upper one corresponds to $\nu \simeq 0.99$. The hatched region is ruled out by Eq. (31). All in all, we obtain the predictions

$$0.16 \lesssim \widetilde{m}/\text{PeV} \lesssim 9.2 \ \text{ with } \ T_{\rm rh}^{\rm max} \simeq 34. \tag{33}$$

These results on $\widetilde{m}$ in conjunction with the necessity for $\mu \sim \widetilde{m}$, established in Sec. 4.2, hint towards the PeV-scale MSSM. Our findings are compatible with the mass of the Higgs boson discovered in LHC [27] for degenerate sparticle spectrum, $1 \le \tan\beta \le 50$ and variable stop mixing.

5. GWs from Metastable CSs

The $U(1)_{\rm R}\times U(1)_{B-L}$ breaking which occurs for $\sigma \simeq \sigma_{\rm c}$ produces a network of CSs which can be considered as metastable due to the embedding of $\mathbb{G}_{\rm L1R}$ in $\mathbb{G}_{\rm LR}$ – see Eq. (5). The dimensionless tension $G\mu_{\rm cs}$ of the CSs produced at the end of FHI can be estimated by [14]

$$G\mu_{\rm cs} \simeq \frac{1}{2}\left(\frac{M}{m_{\rm P}}\right)^2 \epsilon_{\rm cs}(r_{\rm cs}) \ \text{ with } \ \epsilon_{\rm cs}(r_{\rm cs}) = \frac{2.4}{\ln(2/r_{\rm cs})} \ \text{ and } \ r_{\rm cs} = \kappa^2/2g^2 \le 10^{-2}, \tag{34}$$

where we take into account that $(B-L)(\Phi)=1$ in accordance with the coupling in Eq. (7e). Also $G=1/8\pi m_{\rm P}^2$ is the Newton gravitational constant and $g\simeq 0.7$ is the gauge coupling constant at a scale close to M. For the parameters in Eq. (23) we find

$$0.81\lesssim G\mu_{\rm cs}/10^{-8}\lesssim 11. \tag{35}$$

On the other hand, an explanation [6] of the recent NG15 [1, 2] on stochastic GWs entails

$$10^{-8}\lesssim G\mu_{\rm cs}\lesssim 2.4\cdot 10^{-4}\ \text{ for }\ 8.2\gtrsim\sqrt{r_{\rm ms}}\gtrsim 7.5\ \text{ at 95\% c.l.}, \tag{36}$$

where the metastability factor $r_{\rm ms}$ is calculated within our scheme via the relation

$$r_{\rm ms}\simeq m_{\rm M}^2/\mu_{\rm cs}\ \text{ with }\ m_{\rm M}=4\pi M_{W_{\rm R}^\pm}/g^2\ \text{ and }\ M_{W_{\rm R}^\pm}=\sqrt{2}gv_{\rm R}. \tag{37}$$

Here $m_{\rm M}$ is the mass of MMs and $M_{W_{\rm R}^\pm}$ the mass of the gauge bosons. Both are generated by the SSB of $\mathbb{G}_{\rm LR}$ in Eq. (5). Part of the $G\mu_{\rm cs}$ values above can be obtained for

$$1.1\lesssim M/\text{YeV}\lesssim 2.72\ \text{ and }\ 3\lesssim\kappa/10^{-4}\lesssim 14. \tag{38}$$

Fixing $r_{\rm ms}^{1/2}=8$, the M values above provide a prediction for the $v_{\rm R}$ values

$$1\leq v_{\rm R}/\text{YeV}\leq 2.86\ \text{ for }\ 0.9\leq M/\text{YeV}\leq 2.56. \tag{39}$$

Therefore, a significant proximity between $v_{\rm R}$ and M is requested.

Moreover, the GWs obtained from the CSs have to be consistent with the upper bound on their abundance $\Omega_{\rm GW}h^2$ originating from the advanced LVK third observing run [29]

$$\Omega_{\rm GW}h^2(f_{\rm LVK})\lesssim 1.7\cdot 10^{-8}\ \text{ for }\ f_{\rm LVK}=25\ \text{Hz} \tag{40}$$

which implies $G\mu_{\rm cs}\lesssim 2\cdot 10^{-7}$. The long-lasting matter domination obtained in our set up due to the z oscillations after the end of FHI – see Sec. 4.2 – facilitates the fulfillment of the bound above.

Applying the formulae of Ref. [18, 28] we compute $\Omega_{\rm GW}h^2$ for the GWs produced from the CS formatted in our setting under the assumption that these are metastable. Employing the model parameters of Table 2 – which yields $G\mu_{\rm cs}=7.4\cdot 10^{-8}$ – we obtain the outputs displayed in Fig. 3. Namely, in Fig. 3-(a) we show $\Omega_{\rm GW}h^2$ as a function of f for $r_{\rm ms}^{1/2}=8$ and $\mu=\widetilde{m}/3$ which yields $T_{\rm rh}=0.4$ GeV (dotted line) or $\mu=3\widetilde{m}$ which results to $T_{\rm rh}=3$ GeV (solid line) – see Table 2. On the other hand, for the GW spectra depicted in Fig. 3-(b) we employ $\mu=\widetilde{m}$ resulting to $T_{\rm rh}=1.03$ GeV and fix $r_{\rm ms}^{1/2}$ to 7.9 (dotted line) 8 (solid line) and 8.2 (dashed line) – see Eq. (36). In both panels of Fig. 3 we see that the derived GW spectra can explain the NG15 shown with gray almost vertical lines. We see though that, as $r_{\rm ms}^{1/2}$ increases, the increase of $\Omega_{\rm GW}h^2$ becomes sharper and provide better fit to the observations. Also, in both panels the shape of GW signal suffers a diminishment above a turning frequency $f_{\rm rh}\sim 0.03$ Hz which enables us to satisfy Eq. (40) more comfortably than in the case with high reheating. As $T_{\rm rh}$ decreases, the reduction of $\Omega_{\rm GW}h^2$ becomes more drastic in accordance with the findings of Ref. [28]. The plots also show examples of sensitivities of possible future observatories which can test the signals at various f values – see Ref. [18, 20] and references therein.

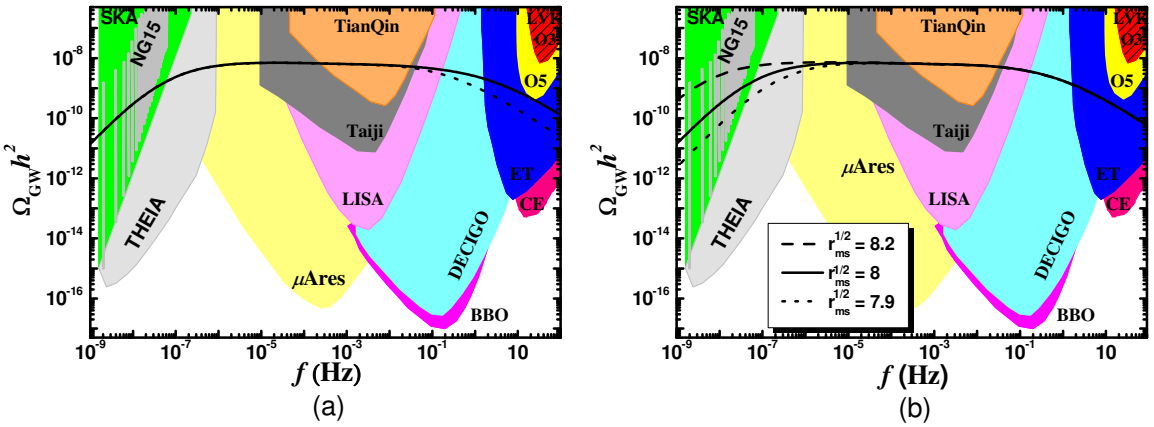

Figure 3: *GW spectra from metastable CSs for (a)* $r_{\rm ms}^{1/2} = 8$ *and* $\mu = \widetilde{m}/3$ *(dotted line) or* $\mu = 3\widetilde{m}$ *(solid line) (b)* $\mu = \widetilde{m}$ *and various* $r_{\rm ms}^{1/2}$ *indicated in the plot. The remaining inputs are taken from Table 2. The shaded areas in the background indicate the sensitivities of various current and future experiments – see Ref.* [18] *and references therein.*

6. Conclusions

We analyzed the production of CSs within a $\mathbb{G}_{\rm L1R}$-invariant model which incorporates FHI and SUSY breaking consistently within an approximate R symmetry. The CSs may be metastable due to preinflationary GUT genealogy – see Eq. (5). The model offers the following interesting, in our opinion, achievements:

- Observationally acceptable FHI adjusting the tadpole parameter a_S and the $\mathbb{G}_{\rm L1R}$ breaking scale M as shown in Eq. (23);
- A prediction of the SUSY-mass scale $\widetilde{m}$ which turns out to be of the order of PeV;
- Generation of the μ term of MSSM with $|\mu| \sim m_{3/2}$;
- An interpretation of the DE problem without extensive tuning;
- Compatibility of the reheating temperature $T_{\rm rh}$ with BBN;
- An explanation of the NG15 via the decay of the CSs.

Due to the low $T_{\rm rh}$ our proposal faces difficulties with the following issues:

- Baryogenesis. An interesting possibility is to take advantage from the non-thermal decay of sgoldstino within some modified version of MSSM – cf. Ref. [30].
- Cold-dark-matter abundance. The relic density of the lightest neutralino although in the PeV range may be inadequate to account for the dark-matter abundance. Non-thermal contribution [31] from gravitino decay may be welcome for this aim.

References

[1] J. Antoniadis *et al.* [EPTA Collaboration] *The second data release from the European Pulsar Timing Array - III. Search for gravitational wave signals, Astron. Astrophys.* **678**, A50 (2023) [arXiv:2306.16214].

[2] G. Agazie *et al.* [NANOGrav Collaboration], *The NANOGrav 15 yr Data Set: Evidence for a Gravitational-wave Background*, *Astrophys. J. Lett.* **951**, no. 1, L8 (2023) [arXiv:2306.16213].

[3] Y. Akrami *et al.* [*Planck* Collaboration], *Planck 2018 results. X. Constraints on inflation*, *Astron. Astrophys.* **641**, A10 (2020) [arXiv:1807.06211].

[4] T. Louis *et al.* [ACT Collaboration], *The Atacama Cosmology Telescope: DR6 Power Spectra, Likelihoods and ΛCDM Parameters*, arXiv:2503.14452.

[5] G. Aad *et al.* [ATLAS Collaboration], *Phys. Rev. D* **90**, 052004 (2014); CMS Collaboration, Tech. Rep. CMS-PAS-HIG-14-009 (2014).

[6] A. Afzal *et al.* [NANOGrav Collaboration], *The NANOGrav 15 yr Data Set: Search for Signals from New Physics*, *Astrophys. J. Lett.* **951**, no. 1, L11 (2023); *ibid.* **971**, no. 1, L27 (2024) [arXiv:2306.16219].

[7] R. Jeannerot, J. Rocher and M. Sakellariadou, *How generic is cosmic string formation in SUSY GUTs, Phys. Rev. D* **68**, 103514 (2003) [hep-ph/0308134].

[8] W. Buchmüller, *Metastable strings and dumbbells in supersymmetric hybrid inflation*, *J. High Energy Phys.* **04**, 168 (2021) [arXiv:2102.08923].

[9] W. Ahmed, T.A. Chowdhury, S. Nasri and S. Saad, *Gravitational waves from metastable cosmic strings in Pati-Salam model in light of new pulsar timing array data, Phys. Rev. D* **109** (2024) 015008 [arXiv:2308.13248].

[10] G.R. Dvali, Q. Shafi and R.K. Schaefer, *Large scale structure and supersymmetric inflation without fine tuning*, *Phys. Rev. Lett.* **73**, 1886 (1994) [hep-ph/9406319].

[11] G. Lazarides, *Supersymmetric hybrid inflation,* hep-ph/0011130.

[12] C. Pallis, *Reducing the spectral index in F-term hybrid inflation,* Edited by T.P. Harrison and R.N. Gonzales (Nova Science Publishers Inc., New York, 2008) [arXiv:0710.3074].

[13] V.N. Şenoğuz and Q. Shafi, *Reheat temperature in supersymmetric hybrid inflation models*, *Phys. Rev. D* **71**, 043514 (2005) [hep-ph/0412102].

[14] C. Pallis and Q. Shafi, *Update on Minimal Supersymmetric Hybrid Inflation in Light of PLANCK*, *Phys. Lett. B* **725**, 327 (2013) [arXiv:1304.5202].

[15] W. Buchmüller, V. Domcke, K. Kamada and K. Schmitz, *Hybrid Inflation in the Complex Plane, J. Cosmol. Astropart. Phys.* **07**, 054 (2014) [arXiv:1404.1832].

[16] M.U. Rehman and Q. Shafi, *Supersymmetric Hybrid Inflation in light of Atacama Cosmology Telescope Data Release 6, Planck 2018 and LB-BK18,* arXiv:2504.14831.

[17] G. Lazarides and C. Pallis, *Probing the Supersymmetry-Mass Scale With F-term Hybrid Inflation*, *Phys. Rev. D* **108***, no. 9,* 095055 (2023) [arXiv:2309.04848].

[18] C. Pallis, *PeV-Scale SUSY and Cosmic Strings from F-Term Hybrid Inflation, Universe* **10**, no. 5, 211 (2024) [arXiv:2403.09385].

[19] C. Pallis, *SUSY-breaking scenarios with a mildly violated R symmetry, Eur. Phys. J. C* **81**, no. 9, 804 (2021) [arXiv:2007.06012].

[20] C. Pallis, *T-model Higgs inflation and metastable cosmic strings, J. High Energy Phys.* **01**, 178 (2025) [arXiv:2409.14338].

[21] M.N. Ahmad, M. Mehmood, M.U. Rehman and Q. Shafi, *μ-Hybrid Inflation and Metastable Cosmic Strings in $SU(3)_c \times SU(2)_L \times SU(2)_R \times U(1)_{B-L}$*, *Phys. Rev. D* **111**, no. 8, 8 (2025) [arXiv:2501.06307].

[22] K.J. Bae, H. Baer, V. Barger and D. Sengupta, *Revisiting the SUSY μ problem and its solutions in the LHC era, Phys. Rev. D* **99**, no. 11, 115027 (2019) [arXiv:1902.10748].

[23] K.J. Bae, H. Baer, V. Barger and R.W. Deal, *The cosmological moduli problem and naturalness*, *J. High Energy Phys.* **02**, 138 (2022) [arXiv:2201.06633].

[24] J. Ellis, M. Garcia, D. Nanopoulos and K. Olive, *Phenomenological Aspects of No-Scale Inflation Models*, *J. Cosmol. Astropart. Phys.* **10**, 003 (2015) [arXiv:1503.08867].

[25] T. Hasegawa *et al.*, *MeV-scale reheating temperature and thermalization of oscillating neutrinos by radiative and hadronic decays of massive particles*, *J. Cosmol. Astropart. Phys.* **12**, 012 (2019) [arXiv:1908.10189].

[26] M. Endo *et al.*, *Moduli-induced gravitino problem*, *Phys. Rev. Lett.* **96**, 211301 (2006) [hep-ph/0602061].

[27] E. Bagnaschi, G.F. Giudice, P. Slavich and A. Strumia, *Higgs Mass and Unnatural Supersymmetry, J. High Energy Phys.* **09**, 092 (2014) [arXiv:1407.4081].

[28] P. Auclair *et al.*, *Probing the gravitational wave background from cosmic strings with LISA, J. Cosmol. Astropart. Phys.* **04**, 034 (2020) [arXiv:1909.00819].

[29] R. Abbott *et al.* [KAGRA, Virgo and LIGO Scientific], *Upper limits on the isotropic gravitational-wave background from Advanced LIGO and Advanced Virgo's third observing run, Phys. Rev. D* **104**, no. 2, 022004 (2021) [arXiv:2101.12130].

[30] R. Allahverdi, B. Dutta and K. Sinha, *Baryogenesis and Late-Decaying Moduli, Phys. Rev. D* **82**, 035004 (2010) [arXiv:1005.2804].

[31] D.J.H. Chung, E.W. Kolb and A. Riotto, *Nonthermal supermassive dark matter*, *Phys. Rev. Lett.* **81**, 4048 (1998) [hep-ph/9805473].